JOURNAL OF NANO- AND ELECTRONIC PHYSICS
Vol. **10** No 4, 04001(5pp) (2018)

ЖУРНАЛ НАНО- ТА ЕЛЕКТРОННОЇ ФІЗИКИ
Том **10** № 4, 04001(5cc) (2018)

Impact of Sputtering Pressure on Structural, Optical, Electrical and Morphological Properties of Titanium Doped Zinc Oxide Thin films Using Metallic Target

F. Bouaraba[1,*], M.S. Belkaid[1], S. Lamri[2]

[1] *Laboratory of Advanced Technologies of Genie Electrics (LATAGE), Mouloud Mammeri University (UMMTO), BP N° 17 15000 Tizi Ouzou, Algeria*
[2] *ICD-LASMIS, University of Technology of Troyes, UMR 6281, CNRS, Technological Pole of Haute-Champagne, 52800 Nogent, France*

(Received 11 April 2018; published online 25 August 2018)

Transparent Titanium Zinc oxide (TZO) thin films with interesting properties have been successfully deposited on silicon and glass substrate by direct current reactive magnetron co-sputtering at room temperature using inexpensive metallic target materials as compared to the high production cost of ceramic target materials. The aim of this work is to study the effects of sputtering pressure on crystallinity, surface morphology, electrical and optical properties of the films, for that a variety of characterization techniques are used. The X-ray diffraction (XRD) results show that films are highly crystalline with a hexagonal wurtzite structure, the microstructure of the films was investigated by scanning electron microscopy (SEM), the energy dispersive x-ray spectrometer (EDS) confirmed the existence of Zn, O and Ti in the deposited films. The electrical resistivity and the transmittance of the films were measured using four point probe method and ultraviolet-visible spectrophotometer (UV-Vis) respectively. The film deposited at 1Pa showed the lowest electrical resistivity of $1.45 \cdot 10^{-3}$ Ω·cm and a very high transmittance above 90 %, it is therefore a good candidate for it application as transparent electrodes in photovoltaic cells.

Keywords: Thin Films, Ti doped ZnO, Sputtering Pressure, Magnetron co-sputtering, Metallic Target.

DOI: 10.21272/jnep.10(4).04001 PACS numbers: 68.60.Bs, 73.61.Ph, 78.66.Bz

1. INTRODUCTION:

In recent times, transparent conductive oxide (TCO) with low specific resistance and high transparency in the visible region has become the subject of intense investigation for large area electronics devices such as solar cells, flat panel display, piezoelectric sensors and touch screens [1, 2].

Among the different TCO materials, Zinc oxide has received increasing attention in the research community due to its abundant, low cost, wide band gap (3.3-3.4 eV) in the near ultraviolet region[3, 4], good stability in hydrogen plasma process, and non toxicity[5].

Many dopants such as Gallium (Ga) [6, 7], Aluminum (Al) [8, 9], Copper (Cu) [10], Boron (Br) [11] Indium (In) [12], and Magnesium (Mg) [13], etc., have been used to improve the electrical conductivity of ZnO, we used Ti as the dopant because it becomes Ti^{+4} when it substitutes the Zn^{2+} site in the ZnO crystal structure resulting in two more free electrons to contribute for electric conduction [14]. Furthermore, Ti has radius of 6.8 nm, which could be incorporated as an interstitial atom, and acts as a scattering site in ZnO, where Zn has a radius of 7.4 nm[15].

Among several technologies used to prepare transparent conductive zinc oxide [16, 17],the magnetron co sputtering process is attractive due to the controllability of composition, it is well adapted to the production of large industrial area surfaces with significant cost reductions[18], thus gives an alternative for the use of expensive ceramic compound targets.

The aim of this work is the elaboration of TZO thin films with good structural, optical, electrical and morphological properties and to study the influence of sputtering pressure on the proprieties of the films in order to find the moderate sputtering pressure to consider the application of these films as transparent electrode in solar cells.

2. EXPIREMENTAL DETAILS

Titanium doped zinc oxide (TZO) thin films were deposited by DC magnetron co sputtering technique using Plasyss system. High purity metal targets of Zn (99.99 %) and Ti (99.99 %) with (10 cm) width, (20 cm) length and (0.6 mm) thickness, are used.

The base pressure in chamber was ($6.7 \cdot 10^{-6}$ mbar). The glass and silicon substrate were ultrasonically cleaned in acetone and ethanol to remove grease and organic contamination and finally rinsed in an ultrasonic bath in deionized water for (15 min), with drying in hot air before deposition.

Argon and oxygen gaz, with high purity (99.99 %) were imported into the chamber. The target was presputtered for (15 min) to clean the target surface. The main deposition conditions are summarized in (Table 1).

The crystalline structure of the TZO films was analyzed by an X-ray diffraction (XRD) spectroscopy (Bruckers D8 Advance) with a Cu-Kα_1 source (λ = 1.5418 A°). The atomic percentage of Ti in the films is semi quantitatively determined by energy dispersive X-ray spectrometer EDS (SNE 3200M). Optical transmittance characteristics were measured by an ultraviolet-visible (UV-vis) spectrophotometer (UV-1102M241). The surface structure was observed by scanning electron microscopy (SEM) ultra high resolution (FE-SEM SU8030 HITACHI).

* fazia.bouaraba24@hotmail.com

The roughness of the films was characterized by profilometric measurements (AltiSurf 500). Electrical sheet resistance was determined from the four –point probe method.

Table 1 – Main deposition conditions

Parameters	Values
Working Pressure	(0.5, 1, 2, 4) Pa
Sputtering power of Zn	260 W
Sputtering power of Ti	630 W
Sputtering Time	45 min
Target-substrate distance	9.5 cm
Substrate Temperature	Ambient
O_2 flow rate	10 sscm

3. RESULTS AND DISCUSSIONS

3.1 Crystallographic Structure

The structural characteristics were studied on deposited layers at different sputtering pressure (0.5 Pa, 1 Pa, 2 Pa, 4 Pa), as shown in (Fig. 1), all diffractograms have a main peak around (34.3°), this peak shows a privileged orientation of the structure growth along the crystallographic c-axis (002), no others phases were observed, this implies that titanium atoms may replace zinc atomic sites. It can be noted that the intensity of (002) peak increase with the sputtering pressure until 1Pa and decrease with further increasing in the deposition pressure.

This effect is due to the number of collisions that a species undergoes in the plasma, so for low pressures, the particles have significant mean free path and arrive on the substrate with the energy they had when leaving the target, as the sputtering pressure increases the probability of collisions between sputtering particle increases and the species reaching the substrate with negligible energy causes a decrease in crystallization.

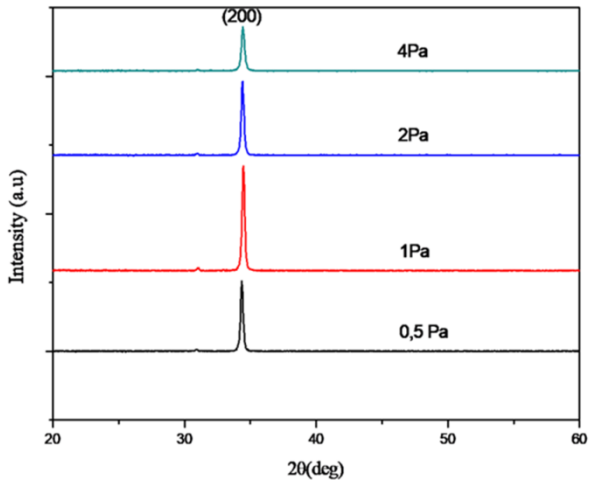

Fig. 1 – XRD patterns for TZO films deposited at different sputtering pressure

3.2 Thicknesses and Deposition Rate

(Fig. 2) showed thicknesses and the deposition rate of TZO films under different sputtering pressure at growth time of 40 min. The result show that as the deposition pressure increases, the growth rate increase, reaches the maximum value of (11.73 nm·min^{-1}) at the deposition pressure of 1 Pa and then decrease with further increasing in the deposition pressure. This result is consistent with the fact that the sputtering pressure determines the flux and energy of neutral species leaving the target, so at higher pressure, the flow of particles reaching the substrate increase, resulting the increase in growth rate

However, a clear decrease in the growth rate is observed as the deposition pressure increases from 1 to 4Pa, it can be attributed to strong collisions between different particles leading to a lower growth rate.

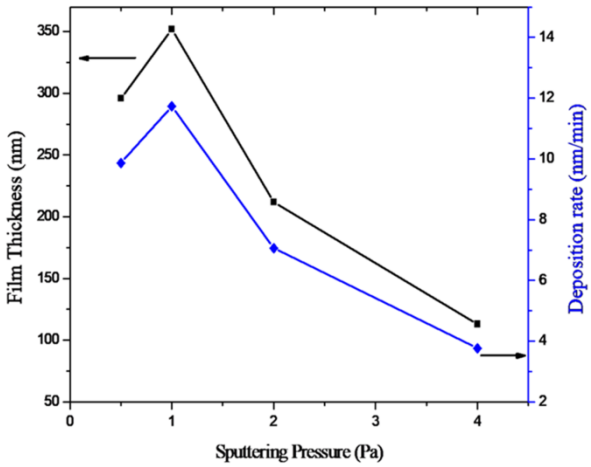

Fig. 2 – Film thickness and deposition rate as a function of varying sputtering pressure

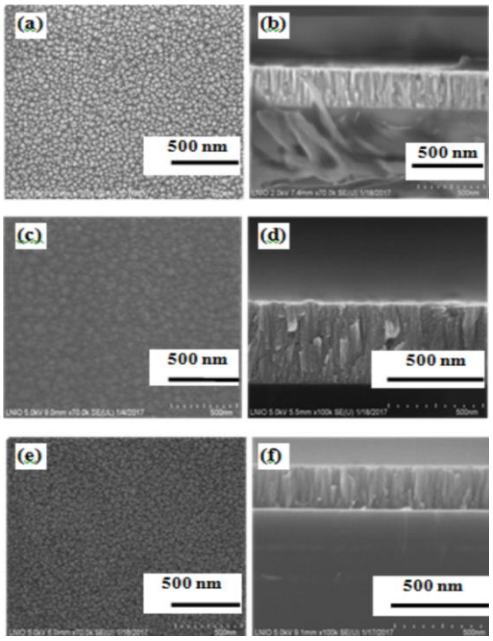

Fig. 3 – Surface and fracture cross section morphologies of TZO thin films: (a. b) 0.5 Pa, (c. d) 1 Pa, (e. f) 4 Pa

3.3 Morphological Characterization

Fig. 3 shows the SEM top surface images and fracture cross section morphologies of the TZO thin films at various sputtering pressure, These images indicate that the layers have a granular structure, and we notice a

increase in the average size of the grains with the increase of the pressure from 0.5 to 1 Pa. however, a higher gas pressure deteriorates preferred orientation of the growth of crystalline films, resulting in a small grain size. We can explain this effect by the energy of the particles, in fact when the particle on the substrate finds a great energy, they reach the favorable recording sites , reducing so the surface irregularities and the density of grain boundaries and allow the formation of large grains sizes

3.4 The surface Roughness

The Roughness is an important element for the application of TZO films in solar cells. Indeed, a rough surface convert the diffusion of the light more effectively and which allows to have more efficient cells.

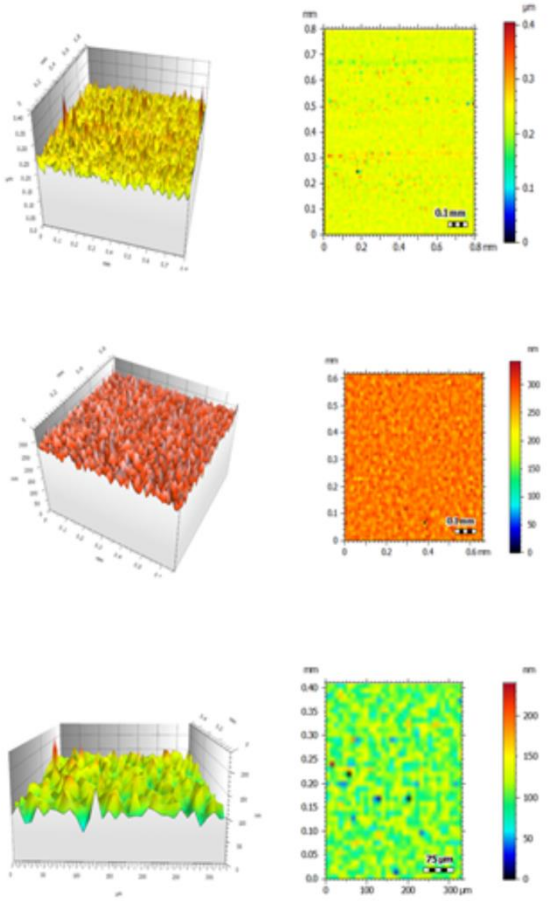

Fig. 4 – The roughness surface of TZO thin films at different sputtering pressure

The changes in the surface Roughness of TZO films at different sputtering pressures were investigated from the profilometer images shown in Fig. 4. It revealed that as sputtering pressure increased from 0.5 Pa to 1 Pa the average surface roughness of the TZO film increased from 17.37 nm to 25.24 nm and the granular structure of the deposited films enhanced, as the deposition pressure increase to 4 Pa the average surface roughness decrease to 13.32 nm, this decrease could be described as a consequence of reduction in grain size wish is in good accordance with SEM results.

3.5 Chemical Characterization

Concerning the composition in elements, the energy dispersive x-ray spectrometer (EDS) analysis (Fig. 5) confirm the presence of Titanium in the crystalline ZnO thin films.The presence of the constituent elements : Zn, O and Ti were confirmed by the occurrence of their respective peaks. As the layers have a small thickness, the Si present in the substrate was detected.

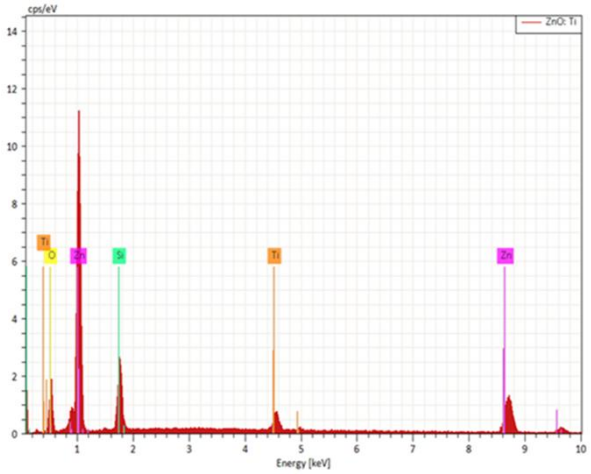

Fig. 5 – The EDX spectra of TZO thin films

Fig. 6 shows the Ti atomic percentage in the zinc oxide films at deferent pressure, it can be seen that the titanium atoms were effectively incorporated into the zinc oxide films.

Ti atomic percentage increase, reaches the maximum value at the deposition pressure of 1 Pa, and then decreases with further increase in the deposition pressure, because only high kinetic energy of titanium atoms can be effectively incorporated into lattice of ZnO crystal.

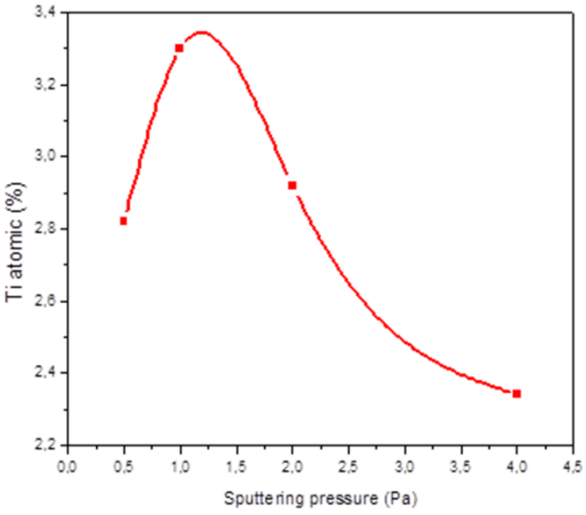

Fig. 6 – Ti atomic percentage in the TZO thin films

3.6 Optical Characterization

The graph of Fig. 7 represents the different transmission spectra of the deposited samples as a function of the sputtering pressure. All spectra demonstrate high transparency in the visible range (400 nm-

800 nm) with a average transmittance around 90 % for each film. From the figure, interference can be observed for all the samples; this observation shows a fairly homogeneous film thickness.

The relationship between the optical band gap and absorption coefficient is given by the Tauc model [19]:

$$\alpha h\nu \propto (h\nu - E_g)^{\frac{1}{2}}, \quad (1)$$

where h is the Planck constant, E_g is the optical gap and ν is the frequency of incident photon.

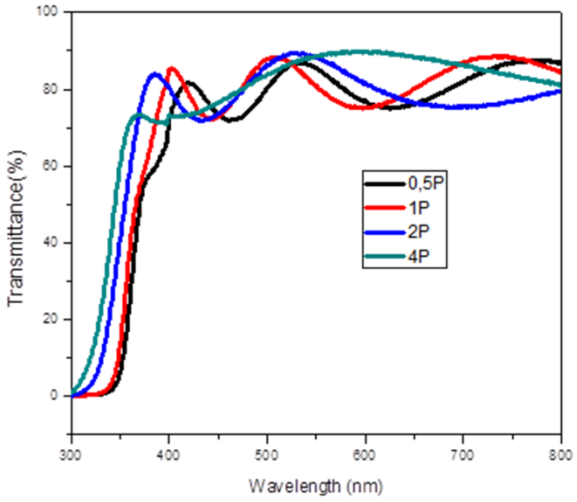

Fig. 7 – Optical transmittance spectra of TZO films at different sputtering pressure

The optical gap is deduced from the square curve of the absorption coefficient and the photon energy $(\alpha h\nu)^2$ as a function of the energy of the photon $(h\nu)$ by extrapolating the curve to the energy axis, the absorption coefficient (α) can be evaluated from the spectrum of the transmittance using the formula [20, 19]:

$$\alpha = (\frac{1}{t})\ln(\frac{1}{T}) \quad (2)$$

where t is the thickness and T the optical transmittance.

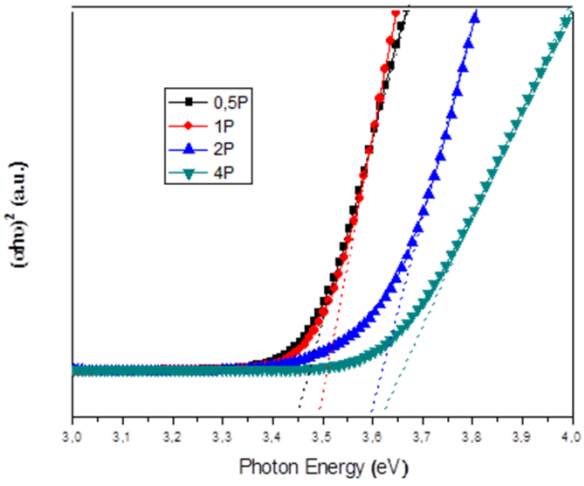

Fig. 8 – Plots of $(\alpha h\nu)^2$ vs photon energy for TZO films prepared at different sputtering pressure

The optical gap of TZO films vary from 3.34 to 3.65 eV with increasing pressure these results are comparable to those given by other authors [22], this increase in optical gap compared to that of pure ZnO is caused by the increase of Fermi level due to the increase of electron concentration after the doping with Ti.

3.7 Electrical Characterization

We show in Fig. 9 the resistivity results, we can see that the electrical resistivity decreases from $3.35{\cdot}10^{-2}$ Ω·cm to $1.45{\cdot}10^{-3}$ Ω·cm as the sputtering pressure increases from 0.5 to 1 Pa and then increases with higher sputtering pressure.

This behavior can be explained by the morphology of the films, it can be seen from Fig. 3 that the crystallite size increases firstly, then decreases and reaches a maximum value at 1 Pa. So as the size of the crystallites increases, the density of the grain boundaries decreases and we can expect an increase in mobility and therefore a decrease in resistivity.

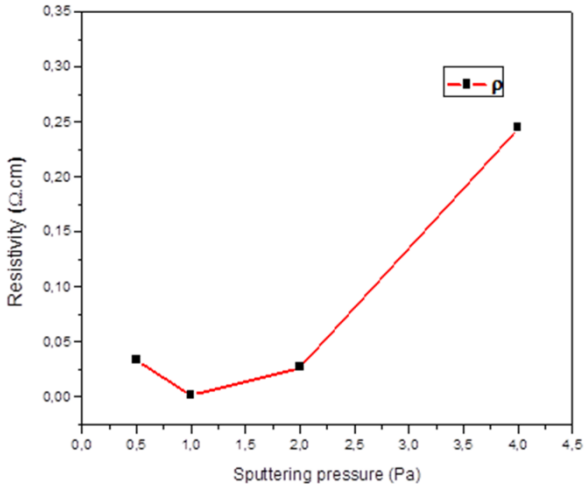

Fig. 9 – Resistivity of TZO films deposited at different sputtering pressure

4. CONCLUSION

In the current work, we studied the impact of sputtering pressure on the structural, optical and electrical properties of the TZO thin films deposited by DC reactive magnetron co sputtering. The structural characterizations show that all the deposited layers have a preferred growth orientation along the c (002) axis perpendicular to the plane of the substrate. Morphological characterization by scanning electron microscopy (SEM) confirmed the structure of growth observed by XRD. The estimated value of optical band gap is from 3.34 to 3.65 eV range and increase with the sputtering pressure. The best optoelectronic performance can be achieved at the sputtering pressure of 1 Pa with average visible transmittance of 90% and the minimal resistivity of $1.45{\cdot}10^{-3}$ Ω·cm. These results can useful for understanding the effects of sputtering pressure on the properties of TZO films, and choosing moderate pressure to obtain high quality TZO films especially for applications as transparent conductive in solar cells.

AKNOWLEDGEMENTS

Authors are grateful to Mr Deturche Regis, Mr Beal Jeremie and Mr Nomenyo Komla (Laboratory of Nano-technology and Optical Instrumentation (LNIO)) for SEM and four point measurements.

REFERENCES

1. J.R.R. Bortoleto, M. Chaves, A.M. Rosa, E.P. da Silva, S.F. Durrant, L.D. Trino, P.N. Lisbo-Filho, *J Appl. Surf. Sci.* **334**, 210 (2015).
2. Y.S. Choi, J.B. Kim, J.G. Han, *Surf. Coat. Technol.* **254**, 371 (2014).
3. Y.F. Zhukovskii, S. Piskunov, O. Lisovski, E. Spohr, R.A. Evarstov, *Phys. Status Solidi B* **253**, 2120 (2016).
4. J.B. Kim, S.B. Jin, L. Wen, P. Premphet, K. Leksakul, J.G. Han, *Thin Solid Films* **587**, 88 (2015).
5. N.H. Como, A. Acevedo, M. Aleman, I. Mejia, M.Q. Lopez, *Microelectron. Eng.* **150**, 26 (2016).
6. S. Lee, D. Cheon, W.J. Kim, M.H. Ham, W. Lee, *J. Appl. Surf. Sci.* **258**, 6537 (2012).
7. K.J. Ahn, J.H. Park, B.K. Shin, W. Lee, G.Y. Yeom, J.M. Myoung, *J. Appl. Surf. Sci.* **271**, 216 (2013).
8. B. Yun Oh, M.C. Jeong, D.S. Kim, W. Lee, J.M. Myoung, *J. Cryst. Growth.* **281**, 475 (2005).
9. Q. Shi, M. Dai, S. Lin, H.J. Hou, C.B. Wei, F. Hu, *Trans. Nonferrous Met. Soc. China.* **25**, 1517 (2015).
10. Y. Liu, H. Liu, Y.Yu, Q. Wang, Y. Li, Z. Wang, *Mater. Lett.* **43**, 319 (2015).
11. D.G. Alonso, S.E. Potts, C.A. A. van Helvoirt, M.A. Verheijen, W.M.M. Kessels, *J. Mater. Chem. C* **3**, 3095 (2015).
12. J.H. Hsieh, C. Li, S.J. Liu, W.S. Lin, *Surf. Coat. Technol.* **228**, S499 (2013).
13. N.H. Hashim, S. Subramani, M. Devarajan, A.R. Ibrahim, *J Aust. Ceram. Soc.* **53**, 421 (2017).
14. T. Akilan, N. Srinivasan, R. Saravanan, *Mater. Sci. Semicond. Proc.* **30**, 381 (2015).
15. W. Zhao, Q. Zhou, X. Zhang, X. Wu, *Appl. Surf. Sci.* **305**, 481 (2014).
16. R. Hong, J. Shao, H. He, Z. Fan, *Appl. Surf. Sci.* **252**, 2888 (2006).
17. J.W. Hoon, K.Y. Chan, J. Krishnasamy, T.Y. Tou, D. Knipp, *J. Appl. Surf. Sci.* **257**, 2508 (2011).
18. Y. Liu, H. Liu, Y. Yu, Q. Wang, Y. Li, Z. Wang, *J Mater. Sci. Semicond. Proc.* **16**, 997 (2013).
19. A. Bedia, F.Z. Bedia, M. Maloufi, B. Benyoucef, *Energy Proc.* **74**, 529 (2015).
20. B. He, J. Xu, H.Z. Xing, C.R. Wang, X.D. Zhang, *J. Superlat. Microstruct.* **64**, 319 (2013).
21. Z.Y. Ye, H.L. Lu, Y. Geng, Y.Z. Gu, Z.Y. Xie, Y. Zhang, Q.Q. Sun, S.J. Ding, *Nanoscale Res.* **8**, 108 (2013).
22. Z.Y. Zhong, T. Zhang, *J. Mater. Lett.* **96**, 237 (2013).